Pulse retrieval in frequency-resolved optical gating based on the method of generalized projections

Kenneth W. DeLong, David N. Fittinghoff, and Rick Trebino

Sandia National Laboratories, MS 9057, Livermore, California 94551-0969

Bern Kohler and Kent Wilson

Department of Chemistry, MS 0339, University of California, San Diego, La Jolla, California 92093

We use the algorithmic method of generalized projections (GP's) to retrieve the intensity and phase of an ultrashort laser pulse from the experimental trace in frequency-resolved optical gating (FROG). Using simulations, we show that the use of GP's improves significantly the convergence properties of the algorithm over the basic FROG algorithm. In experimental measurements, the GP-based algorithm achieves significantly lower errors than previous algorithms. The use of GP's also permits the inclusion of an arbitrary material response function in the FROG problem.

Frequency-resolved optical gating (FROG) permits the measurement of the time-dependent intensity and phase of an ultrashort laser pulse without prior assumptions on the form of the pulse.[1-5] FROG simply involves frequency resolving an autocorrelation-type signal, followed by using an iterative-Fourier-transform-based phase-retrieval algorithm[3,6] to extract the intensity and phase of the laser pulse. By use of various geometries, FROG has been realized in the visible, infrared, and ultraviolet on pulses ranging from 2 nJ to 300 μJ in energy and 40 to 300 fs in duration.[1-5,7-10]

The basic FROG algorithm as originally published[3] yields rapid convergence for many pulses but gives no guarantee of convergence and tends to stagnate for complex pulses. A variety of additional techniques improved convergence, but at a cost in complexity and speed.[11] In this Letter we apply the *method of generalized projections*[12,13] (GP's) to the FROG algorithmic problem. GP's are an extremely powerful technique, yet they enjoy a simple implementation and great intuitive appeal. We show how a new GP-based algorithm generally converges even when the basic FROG algorithm fails. We also demonstrate that, when inverting data with noise (experimental data), GP's outperform the basic FROG algorithm significantly. Finally, we show how the use of GP's permits the inclusion of an arbitrary material response, paving the way for the use of noninstantaneously responding materials in FROG.

In the polarization-gate geometry for FROG (Ref. 2) the FROG signal field takes the form

$$E_{\rm sig}(t,\tau) = E(t)|E(t-\tau)|^2, \qquad (1)$$

where $E(t)$ is the pulse electric field versus time and τ is the delay between the two pulse replicas. The FROG trace is the squared magnitude of the Fourier transform of this signal:

$$I_{\rm FROG}(\omega,\tau) = \left| \int_{-\infty}^{\infty} dt\, E_{\rm sig}(t,\tau)\exp(i\omega t) \right|^2. \qquad (2)$$

The task of the FROG algorithm is to find a signal field $E_{\rm sig}(t,\tau)$ that satisfies two distinct constraints, i.e., the mathematical constraint of Eq. (1) [the ability to be generated from a physically realizable field $E(t)$ through a known nonlinear-optical process] and also the constraint of Eq. (2) (that the magnitude squared of its Fourier transform match the experimentally measured FROG trace).

This situation is illustrated in Fig. 1, which shows that the correct solution lies at the intersection of the two sets of fields that satisfy the two individual constraints. The method of solution based on projections is also diagrammed in Fig. 1. Starting with an arbitrary signal field (which is most likely not in either constraint set), a projection onto the first constraint set is made. A projection of a point onto a set involves moving to the closest point inside the set. We can accomplish this by minimizing a distance metric between the starting point and a general point in the set. From this new point a projection onto the second set is then performed, followed by a projection back onto the first set, etc. By iteratively projecting onto the two sets, we will eventually arrive at the intersection of the two sets, i.e., at the correct answer.
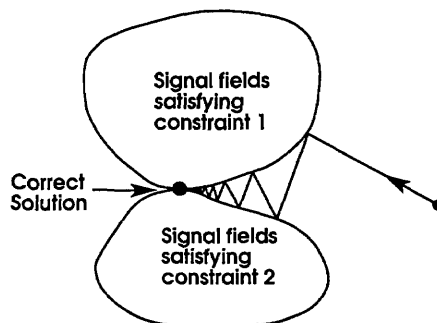

Fig. 1. Schematic of the method of generalized projections. The figure is pedagogical; in FROG the sets (which reside in a higher-dimensional space) may be of a more complicated structure.

The sets shown in Fig. 1 are convex; a line segment between any two points in the set never leaves the set. When both constraint sets are convex, we speak of the method of projections, and convergence is guaranteed. In the case in which one or both of the constraint sets are nonconvex (in this case the method is called GP's), convergence cannot be guaranteed mathematically (the method can become stuck on protrusions in the constraint sets), but the method is often found to work effectively despite this.[12] This is the case for FROG; although both constraint sets are nonconvex, we find that GP's work well in the FROG algorithm.

The details of the basic FROG algorithm were published elsewhere.[3,11] Essentially it involves Fourier transforming the signal field back and forth between the time and frequency domains. The algorithm satisfies the constraint specified by Eq. (2) by replacing the magnitude of the current signal field in the frequency domain by the square root of the intensity $I_{FROG}(\omega, \tau)$ of the experimental FROG trace:

$$E'_{sig}(\omega, \tau) = \frac{E_{sig}(\omega, \tau)}{|E_{sig}(\omega, \tau)|} \sqrt{I_{FROG}(\omega, \tau)}. \qquad (3)$$

Magnitude replacement in this fashion was shown to be a GP.[12]

In previously published algorithms, satisfaction of the constraint indicated by Eq. (1) involved a simple integration and was not a GP. To implement a GP for this constraint in polarization-gate FROG, we instead minimize the following distance metric:

$$Z = \sum_{i,j=1}^{N} \left| E'_{sig}(t_i, \tau_j) - E(t_i) \left| E(t_i - \tau_j) \right|^2 \right|, \qquad (4)$$

where $E'_{sig}(t, \tau)$ is the inverse Fourier transform with respect to ω of $E'_{sig}(\omega, \tau)$. The quantity $E(t)|E(t - \tau)|^2$ is a general point inside the constraint set of Eq. (1) (other FROG geometries would necessitate the use of an appropriately modified distance function[5]). The field $E(t)$ that minimizes Z then forms the field used for the index iteration of the algorithm. In practice a single one-dimensional minimization along the gradient of Z (Refs. 11 and 14) rather than a full multidimensional minimization appears to be sufficient and computationally less expensive [we use as the starting point of the minimization the field $E(t)$ that began the cycle in Eq. (1)].

The double pulse, which consists of the coherent sum of two Gaussian pulses separated by twice their intensity full width at half-maximum, presents considerable problems for the basic FROG algorithm and was used as a test case for a previous study on algorithmic improvements.[11] Figure 2 shows the performance of the basic FROG algorithm, the composite algorithm incorporating the improvements detailed in Ref. 11, and the GP-based FROG algorithm in retrieving the double pulse. Whereas the basic FROG algorithm stagnates at a very high error, the GP-based algorithm successfully and quickly inverts the double-pulse FROG trace. The composite algorithm also inverts the pulse successfully; however,

it is much slower. We find that this observation extends to all pulses with significant intensity substructure; i.e., the GP-based algorithm is successful, the basic FROG algorithm stagnates, and the composite algorithm usually converges but does so more slowly.

In the case of experimental data, in which noise is always present, the only quantitative measure of performance is the rms difference between the experimental FROG trace and the trace of the retrieved field, i.e., the so-called FROG error[11] [when calculating FROG error for GP-retrieved traces, one does not need to normalize the retrieved trace to its peak value; its scale is set by Eq. (4)]. Using this measure, we find that the GP-based algorithm performs significantly better than the basic FROG algorithm on experimental data. On a series of polarization-gate FROG traces of pulses from a regeneratively amplified Ti:sapphire laser system we found that, in 19 of 20 traces, GP's performed better than the basic FROG algorithm. The average reduction in error for these 19 traces was 35%, with the largest reduction being 50%. This improvement is also typical of results with the second-harmonic generation FROG.

In Fig. 3 we see a polarization-gate FROG trace of a pulse from an amplified Ti:sapphire laser. Figure 4 shows the experimentally measured spectrum compared with the spectra of the pulses retrieved by the basic FROG algorithm and the GP-based algorithm. The GP-based algorithm is clearly superior in this instance, providing much closer agreement with the experimental spectrum than does the basic FROG algorithm.

The GP-based algorithm should not, however, entirely supplant the basic FROG algorithm; rather, it appears to complement it. This is because we find that the basic FROG algorithm for pulses that it is able to retrieve converges significantly faster than the GP-based algorithm. For example, in re-
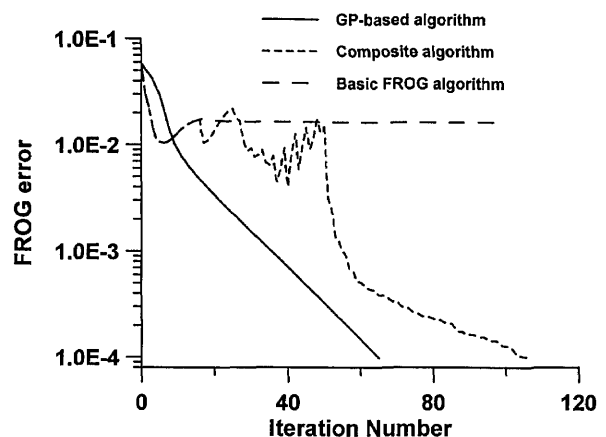

Fig. 2. Error in the retrieved FROG traces as a function of iteration number for the basic FROG algorithm, the composite algorithm, and the new GP-based algorithm for the double pulse. Whereas the basic FROG algorithm stagnates, the GP-based algorithm successfully retrieves this pulse. The composite algorithm also retrieves the pulse, but it is much slower (for iteration numbers larger than 50 the composite algorithm used the minimization method, a much slower method in real time than the basic or the GP-based algorithm).
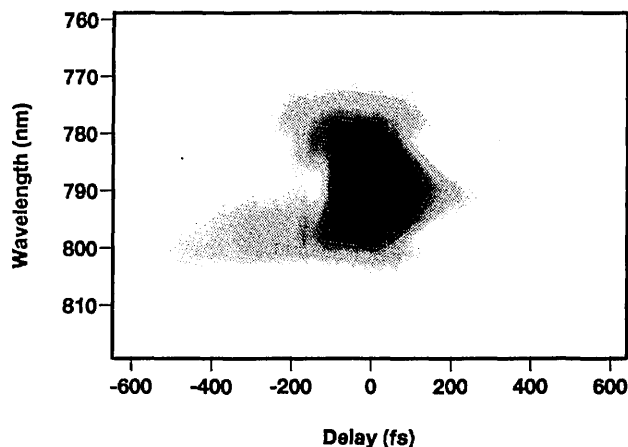
Fig. 3. Polarization-gate FROG trace of an amplified Ti:sapphire laser pulse.
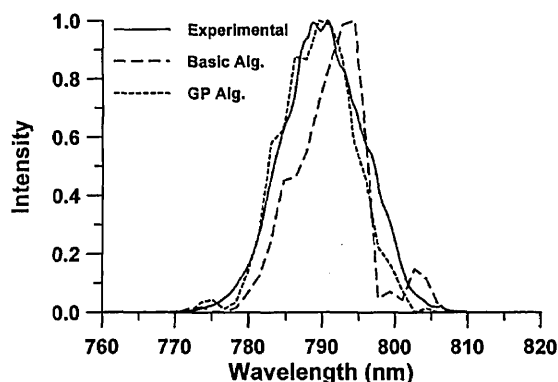

Fig. 4. Spectra retrieved by the basic FROG algorithm (long-dashed curve) and the GP-based algorithm (short-dashed curve) from the trace of Fig. 3 compared with the experimentally measured spectrum (solid curve). Clearly the GP-based algorithm gives better agreement with the experimental spectrum. The final rms error between the experimental and reconstructed traces was 0.0134 for the basic FROG algorithm and 0.00801 for the GP-based algorithm.

trieving a Gaussian pulse with self-phase modulation, although both algorithms converge, the basic FROG algorithm does so significantly faster (20 iterations) than the GP-based algorithm (90 iterations). It is thus generally advantageous to apply the basic FROG algorithm before switching to the GP-based algorithm. An algorithm combining GP's, the basic FROG algorithm, and the other improvements introduced in Ref. 11 yields excellent convergence.

Finally, GP's can be used to include the response of the sample material in FROG. The basic FROG algorithm explicitly assumes an instantaneous material response. However, the use of GP's permits us to include an arbitrary material response function in FROG. We write such an arbitrary material response as

$$E_{\text{sig}}(t, \tau) = f[E(t), \tau], \tag{5}$$

where f can be any response function and may include noninstantaneous terms. To use GP's to retrieve a pulse from a FROG trace generated in a material with the response f, we rewrite the distance metric Z as

$$Z = \sum_{i,j=1}^{N} |E'_{\text{sig}}(t_i, \tau_j) - f[E(t_i), \tau_j]|^2. \tag{6}$$

This new distance metric is minimized with respect to $E(t)$ in the same fashion as Eq. (4) so as to implement the projection onto one of the constraint sets. In this manner, effects such as noninstantaneous response, Raman effects, and saturation can be included in the FROG pulse-retrieval algorithm. This technique opens up a rich new area for FROG that, to our knowledge, has yet to be explored.

References

1. D. J. Kane and R. Trebino, IEEE J. Quantum Electron. **29**, 571 (1993).
2. D. J. Kane and R. Trebino, Opt. Lett. **18**, 823 (1993).
3. R. Trebino and D. J. Kane, Opt. Soc. Am. A **10**, 1101 (1993).
4. D. J. Kane, A. J. Taylor, R. Trebino, and K. W. DeLong, Opt. Lett. **19**, 1061 (1994).
5. K. W. DeLong, R. Trebino, J. Hunter, and W. E. White, J. Opt. Soc. Am. B **11**, 2206 (1994).
6. J. R. Fienup, Appl. Opt. **21**, 2758 (1982).
7. K. W. DeLong, R. Trebino, and D. J. Kane, J. Opt. Soc. Am. B **11**, 1595 (1994).
8. B. Kohler, V. V. Yakovlev, K. R. Wilson, K. W. DeLong, R. Trebino, and J. Squire, Proc. Soc. Photo-Opt. Instrum. Eng. **2116**, 360 (1994).
9. B. Kohler, V. V. Yakovlev, K. R. Wilson, J. Squier, K. W. DeLong, and R. Trebino, in *Ultrafast Phenomena*, Vol. 7 of 1994 OSA Technical Digest Series (Optical Society of America, Washington, D.C., 1994), p. 215.
10. J. Paye, M. Ramaswamy, J. G. Fujimoto, and E. P. Ippen, Opt. Lett. **18**, 1946 (1993).
11. K. W. DeLong and R. Trebino, J. Opt. Soc. Am. A **11**, 2429 (1994).
12. A. Levi and H. Stark, in *Image Recovery: Theory and Applications*, H. Stark, ed. (Academic, San Diego, Calif., 1987) p. 277.
13. E. Yudilevich, A. Levi, G. J. Habetler, and H. Stark, J. Opt. Soc. Am. A **4**, 236 (1987).
14. W. H. Press, W. T. Vetterling, and S. A. Teukolsky, *Numerical Recipes in C: Second Edition* (Cambridge U. Press, Cambridge, 1992), p. 420.